Shape Optimization of Corrugated Coatings Under Grazing Incidence Using a Genetic Algorithm

Hosung Choo, *Student Member, IEEE,* Hao Ling, *Fellow, IEEE,* and Charles S. Liang, *Fellow, IEEE*

***Abstract*—We report on the use of a genetic algorithm (GA) to design optimal shapes for a corrugated coating under near-grazing incidence. A full-wave electromagnetic solver based on the boundary integral formulation is employed to predict the performance of the coating shape. In our GA implementation, we encode each shape of the coating into a binary chromosome. A two-point crossover scheme involving three chromosomes and a geometrical filter are implemented to achieve efficient optimization. Standard magnetic radar absorbing material (MAGRAM) is used for the absorber coating. We present the optimized coating shapes depending on different polarizations. A physical interpretation for the optimized structure is discussed and the resulting shape is compared to conventional planar and triangular shaped designs. Next, we extend this problem from single to multiobjective optimization by using Pareto GA. The optimization results with two different objectives, viz. height (or weight) of the coating versus absorbing performance, are presented.**

***Index Terms*—Coatings, corrugation, genetic algorithms, optimization.**

I. Introduction

LOSSY material coatings are commonly used to reduce scattering from conducting bodies. In general, design of coatings should meet multiple criteria including low reflection, small volume, and light weight. These design goals can conflict with one another. Multilayer planar coatings have been studied extensively for their wideband absorbing characteristics [1], [2]. Recently, genetic algorithms (GA) have been applied with success in finding optimal thicknesses for multilayer coatings in either planar or cylindrical configurations [3]–[5]. Corrugated coatings with nonplanar profiles offer additional degrees of freedom and have been studied in [6]–[10]. In particular, it was shown in [9], [10] that single-material corrugated coating can be exploited to alleviate polarization dependence and improve the absorption performance over a wide range of frequencies at near-grazing incidence. However, only a few simple shapes were considered. In this paper, we use GA to explore more arbitrary coating shapes in an attempt to achieve better absorber performance. With more degrees of freedom in the design, arbitrarily shaped coatings may give rise to better absorbing performance. However, finding an optimal shape is more challenging as the design parameter space is much larger.

Manuscript received April 29, 2002; revised September 13, 2002. This work was supported by the Office of Naval Research under Contract N00014-01-1-0224.

H. Choo and H. Ling are with the Department of Electrical Engineering, University of Texas at Austin, Austin, TX 78712 USA.

C. S. Liang is with the Lockheed Martin Aeronautics Company, Fort Worth, TX 76101 USA.

Digital Object Identifier 10.1109/TAP.2003.818773

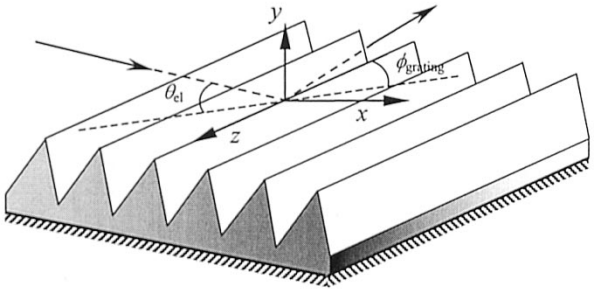

Fig. 1. Geometry of the corrugated absorber.

In our approach, a full-wave electromagnetic simulation code is used to evaluate the absorbing performance of each shape. GA is implemented to optimize the shape of the coating, which is encoded into a binary chromosome. A two-point crossover scheme involving three chromosomes is used as the crossover operator to achieve fast convergence. In addition, geometrical filtering is adopted to create more realizable shapes. In our study, we focus on the near-grazing incidence case. A single-layer MAGRAM material [11] is used as the coating. We first apply this method to achieve optimal shapes under various polarization constraints. (Some preliminary results were reported earlier in [12].) The physical interpretation of the optimized structures is discussed and their performance is compared to the baseline results obtained from conventional planar and triangular shaped designs. Next, we employ the Pareto GA [13], [14] to map the more general set of optimal solutions trading off coating thickness (or weight) versus absorbing characteristics.

This paper is organized as follows. In Section II, we describe the electromagnetic simulation code utilized and other details in our GA implementation. Section III describes the application of the GA to the design of optimal coating shapes under various geometrical and polarization constraints. In Section IV, multiobjective optimization is applied to the design of coating for both absorbing performance and coating thickness. Finally, Section V provides conclusions gathered from this research.

II. Approach

A. EM Simulation Code

The geometry considered in this paper is shown in Fig. 1. The shaped grooves in the coating have a period of p along the x direction and extend to infinity along the z direction. The bottom of the coating is backed by a conducting ground plane. A plane wave is obliquely incident upon the infinite grating with θ_{el} and θ_{grating}.

0018-926X/03$17.00 © 2003 IEEE

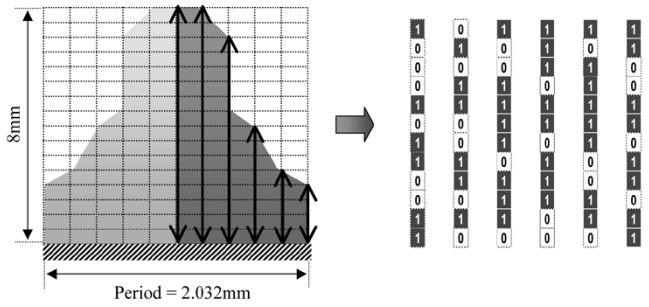

Fig. 2. Encoding of corrugated absorber into a binary chromosome.

To evaluate the performance of each shape for the coating, we use a full-wave electromagnetic code based on a boundary-integral equation formulation [9]. The formulation entails dividing one cell of the grating into different homogeneous regions according to the material layers. A homogeneous Green's function is first used to calculate the moment matrix. Boundary integral equations are then obtained for each region. Field continuity at region interfaces and periodic boundary conditions at cell boundaries are then enforced. The fields in the top half-space are expanded into a sum of Floquet harmonics and are matched to the fields in the lower region so that the reflection coefficients can be found. The code has previously been validated by comparing the simulation results to measurement data in [9], [10].

B. GA Optimization

GAs are stochastic search methods based on the concept of natural selection and evolution [13], [14]. This class of algorithms is particularly attractive for finding an approximate global optimum in a very high-dimensional space. For this reason, we employ GA to optimize the shape of the coating profile. In our GA implementation, each possible absorber shape is encoded into a binary chromosome, as shown in Fig. 2. The period of the absorber is divided into M points. The height of the coating at each point along x is represented as a binary number. A symmetry constraint is applied in the x-direction so that only the right half of the absorber is encoded into the chromosome.

In order to obtain coating shapes that are not too complicated from the manufacturing point of view and to speed up convergence of the GA, a geometrical filter is applied to the chromosomes at each generation of the GA. Two different geometrical filters were tried: a 1-D sliding window filter [15] and a descending order filter. Fig. 3(a) and (b) shows the shapes before and after the 1-D seven-point sliding window filter, which is a low-pass, moving-average filter. As expected, the surface shape after the filtering looks smoother without any sharp peaks. From the results of using this filter, we found that the GA-optimized profiles consistently had shapes that monotonically decreased from a central peak. Therefore, an alternative "descending order filter" was also tried. This filter simply rearranges the height of the absorber at the M points so that the highest point is at the center and all other points are placed in descending order. Fig. 3(c) shows the shape after the descending order filter. Note that this filter preserves the sharp edges in the design while making the shape less oscillatory. We found that the optimized shape from the descending order filter gave better performance than that from the 1-D sliding window filter. Therefore, all the results presented in this paper are generated by using the descending order filter.

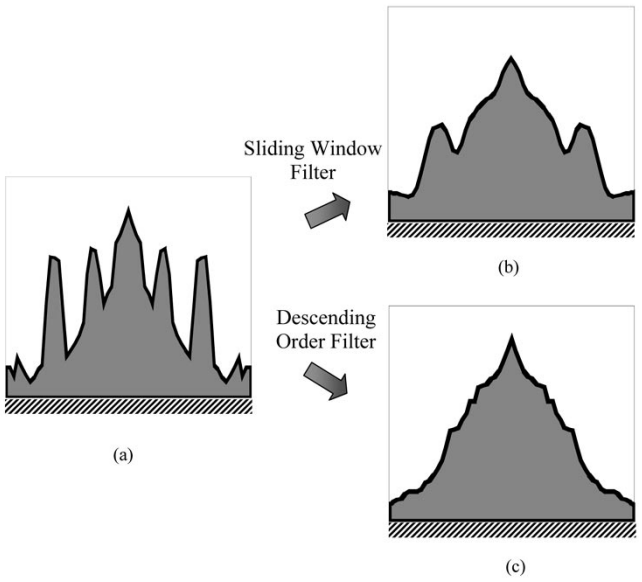

Fig. 3. (a) Before geometrical filter. (b) After seven-point sliding window filter. (c) After the descending order filter.

After these chromosomes are evaluated by the EM simulation code, a cost function related to the absorbing performance is computed. Based on the cost function, chromosomes are refined into the next generation by a reproduction process that involves crossover, mutation and geometrical filtering. For the crossover operation, a two-point crossover scheme involving three chromosomes is used. The process selects three chromosomes as parents and divides each chromosome into three parts. The three parent chromosomes are then intermingled to create three child chromosomes. This series of processes is iterated until the cost function is minimized.

III. GA-Optimized Coating Shapes

In this section, we investigate coating profiles that give rise to the best absorbing characteristic for a given coating height. The design frequency band is chosen to be from 8 to 18 GHz, and the maximum height of the coating is restricted to 8 mm. To avoid higher order diffraction, the period of the coating is set to 2.032 mm. A MAGRAM material is used for the coating (the detailed absorption characteristics can be found in Fig. 7 of [10]). We consider the case when the incident angle is $\theta_{el} = 30^\circ$ and $\phi_{\text{grating}} = 0^\circ$.

To encode each possible shape of the coating into a binary string, we first discretize the period of the coating into 30 points. The height of the groove at each point is described by a 6-bit number (i.e., in 64 steps) that ranges between 0 and 8 mm. When the GA process converges to an optimal value, we increase the discretization for the period and the height to 60 points and 8 bits, respectively, to achieve a more refined coating shape. Associated with the design goal, the cost function is defined as the

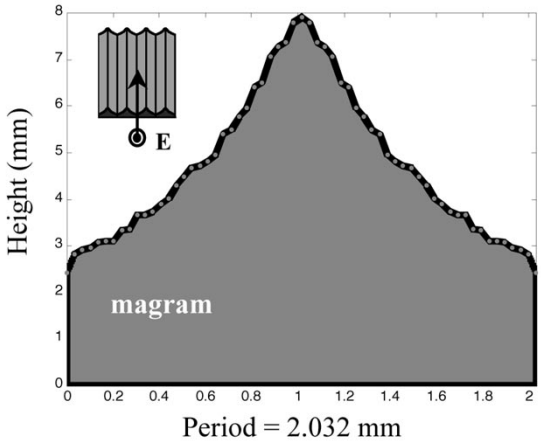

(a)

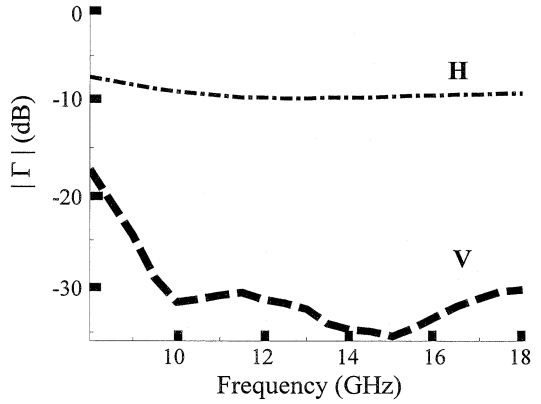

(b)

Fig. 4. (a) GA-optimized shape for the vertical polarization. (b) Reflection coefficient (decibel) versus frequency at 30 degrees from grazing.

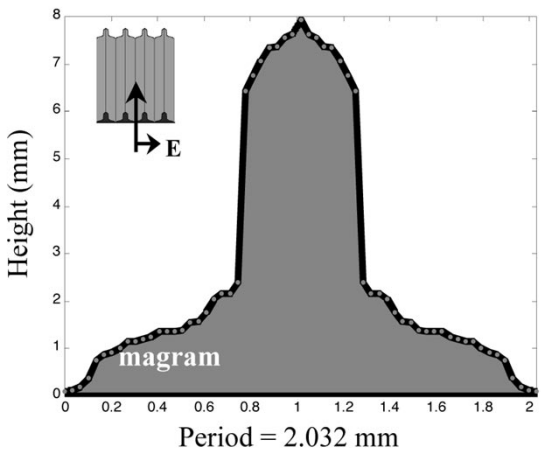

(a)

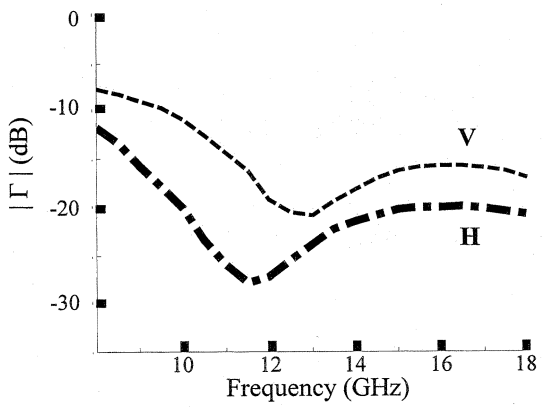

(b)

Fig. 5. (a) GA-optimized shape for the horizontal polarization. (b) Reflection coefficient (decibels) versus frequency.

average of those reflection coefficient values, $\Gamma(\mathrm{dB})$, that exceed -20 dB within the frequency band of interest

$$\text{Cost} = \frac{1}{N}\sum_{n=1}^{N}(P_n) \tag{1}$$

$$\text{where } P_n = \begin{cases} \Gamma(\mathrm{dB}) + 20\ \mathrm{dB}, & \text{if } \Gamma(\mathrm{dB}) \geq -20\ \mathrm{dB} \\ 0, & \text{if } \Gamma(\mathrm{dB}) < -20\ \mathrm{dB} \end{cases}$$

In our GA, the size of the population is chosen to be 30. A crossover probability of 0.8% is used, and the probability of mutation is set to 0.1%. The computational time is about 8 hours on a Pentium IV 1.7 GHz machine for a typical design.

First, we consider the case when only the reflection coefficient for the vertical polarization is used in the cost function definition. Fig. 4(a) shows the resulting GA-optimized shape, which closely resembles a triangular profile. Fig. 4(b) is a plot of the simulated reflection coefficient (in decibels) versus frequency for the optimized shape. We see that the reflection coefficient of the vertical polarization nearly meets the -20 dB design goal over the entire frequency band from 8 to 18 GHz. The horizontal polarization is not optimized and shows a much higher reflection coefficient.

Next, we consider the reverse situation when only the horizontally polarized reflection coefficient is used in the cost function. Fig. 5(a) shows the resulting GA-optimized shape. The optimal shape of the corrugated coating resembles a rectangular profile. Fig. 5(b) shows the associated reflection coefficient (in decibels) versus frequency for the optimized shape. In this case, the reflection coefficient of the horizontal polarization meets the -20 dB design goal for all the frequencies above 10 GHz while the vertical polarization is higher. Further improvement in the low-frequency performance will likely require a thicker coating.

We then compare this optimized shape to the conventional planar and the triangular shaped coatings that are also optimized using GA. The maximum heights of all three coatings are limited to the same 8 mm thickness. Fig. 6 shows the horizontally polarized reflection coefficients for the three coatings. The dashed, solid, and dashed–dotted lines are the respective reflection coefficients for the GA-optimized planar, triangular, and arbitrarily shaped coatings. The planar shaped coating (thickness of 1.19 mm) shows a reflection of about -5 dB within the frequency range of interest. By using the triangular shaped profile (base thickness of 0.03 mm and triangular height of 6.12 mm) the reflection coefficient can be reduced to less than -10 dB. The GA-optimized arbitrarily shaped coating shows better absorbing performance in terms of the cost definition in (1) than either of the conventional designs.

Next, we test the sensitivity of the GA design. To see the effect of different cost definitions, we optimize our design using two

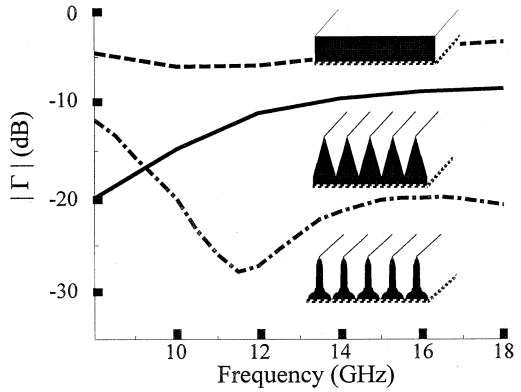

Fig. 6. Performance comparison of the planar absorber (– – – – ––), triangular shaped absorber (——), and GA-optimized absorber (– · – · – · –) for the horizontal polarization.

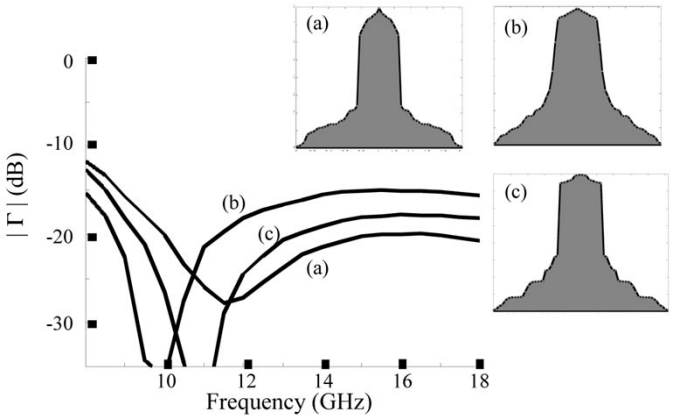

Fig. 7. Effect of cost definitions on the optimization results for the horizontal polarization. (a) Cost definition in (1). (b) Minimax cost definition. (c) Average power reflection coefficient cost definition.

other cost functions. The first alternative cost is the maximum reflection value across the whole frequency range of interest (typically called the Minimax cost function). The resulting performance is indicated by the dashed line in Fig. 7. The second alternate cost function is the averaged power reflection coefficient (on a linear scale) across the frequency band. This design's performance is shown as the dash-dotted line. Some difference in the overall performance is noted. However, we observe that the optimized shapes retain the overall feature of the original design based on the cost definition in (1). To test the sensitivity of the GA-optimized shape to manufacturing tolerances, we introduce random RMS deviations of 0.4 mm into the profile height. The resulting performance is shown in Fig. 8(a) by the dashed line. We also intentionally undersample the 60-point GA description of the profile by a factor of 6, resulting in a more smoothed-out profile. The performance is shown by the dashed–dotted line. We see that the performance is not too sensitive to the deviation to the optimized profile. Fig. 8(b) shows the performance of the optimized coating for close-by incident angles of 25° and 35°. The results indicate some degradation toward the smaller grazing angles.

We also try to optimize the coating shape for both polarizations by using the average of the reflection coefficients from the horizontal and vertical polarizations in the cost function. The resulting shape is shown in Fig. 9(a). As can be seen from the

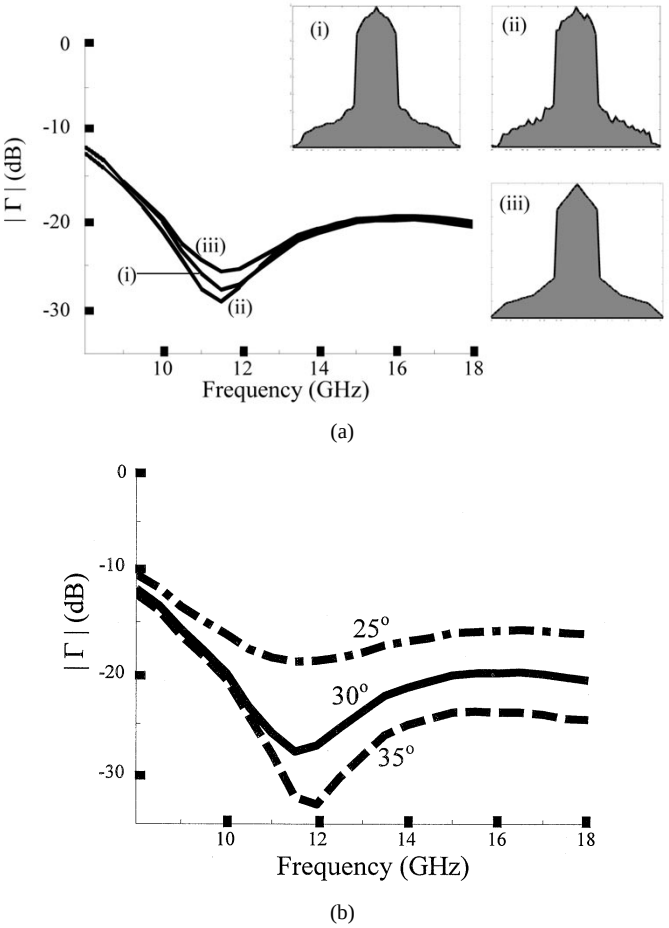

Fig. 8. (a) Performance sensitivity to variations in the shape of the profile for the horizontal polarization. (i) Original GA-optimized design. (ii) GA-optimized shape with rms error of 0.4 mm. (iii) Smoothed shape after 6:1 undersampling. (b) Performance of the optimized coating for close-by incident angles of 25° and 35°

previous examples, the design for the horizontal polarization is more difficult than that for the vertical polarization. Therefore, in this case, the cost is dominated by the horizontal polarization and the resulting GA-optimized shape is not that different from that for the horizontal polarization shown in Fig. 5(a).

Finally, an interpretation on the operating principle of the GA optimized shape is attempted. The left side of Fig. 10 is a planar absorber. Typically it is more difficult for the horizontal polarization to infiltrate an absorber near grazing than the vertical polarization. However, if we look at the incident electric field on the near-vertical sidewalls of the profile shown on the right side of Fig. 10, it behaves more like the vertical polarization. Thus, the absorbing performance is improved by effectively changing the horizontal polarization into the vertical polarization. This explains why our optimized design for the horizontal polarization resembles a rectangular profile. Other researchers have discussed the difference in coupling into corrugated profiles depending on polarization [16].

IV. Multiobjective Optimization

A. Pareto GA and Cost Function Definition

In addition to the absorbing performance of the coating, another design criterion of interest is the coating volume, which

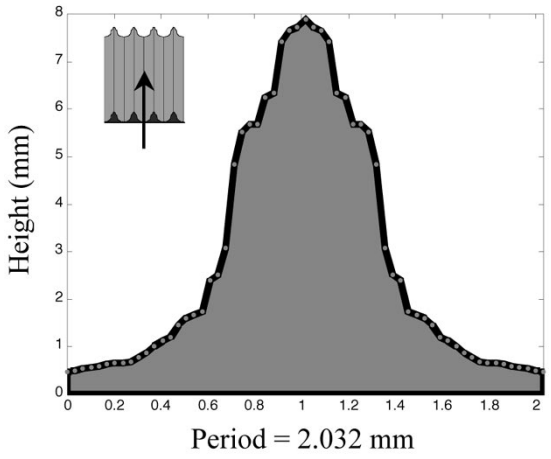

(a)

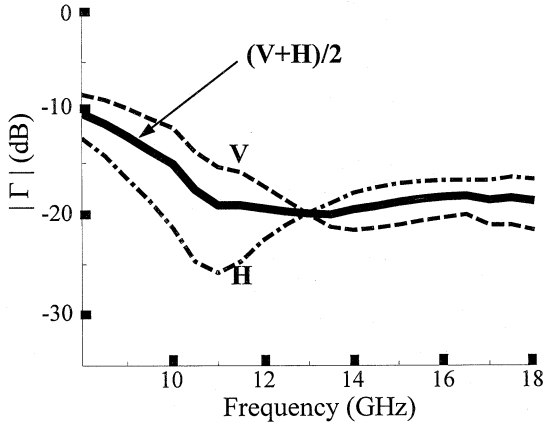

(b)

Fig. 9. (a) GA-optimized shape taking into account of both the vertical and horizontal polarizations. (b) Reflection coefficient (decibels) versus frequency.

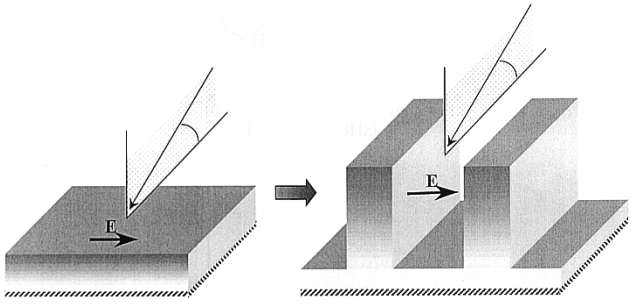

Fig. 10. (a) Planar absorber with horizontal polarized wave incidence. (b) Rectangular profile with horizontal polarized wave incidence.

is measured by the coating height. An investigation of the absorbing performance versus the coating height is studied. This can be done by repeatedly using the same methodology described in Section III for various heights. However, it is much more efficient to cast this problem into a multiobjective problem rather than using the conventional GA. Pareto GA [13], [14] is a useful tool for this problem. In the Pareto GA, a wide range of solutions corresponding to more than one objective can be mapped by running the optimization only once. In our implementation, we define two cost functions:

$$\text{Cost1} = \text{Normalized coating height} \tag{2}$$

$$\text{Cost2} = \text{Normalized value of} \frac{1}{N}\sum_{n=1}^{N}(P_n) \tag{3}$$

where P_n

$$= \begin{cases} \frac{(\Gamma_\perp + \Gamma_\parallel)}{2}(\text{dB}) + 20\ \text{dB}, & \text{if } \frac{(\Gamma_\perp + \Gamma_\parallel)}{2}(\text{dB}) \geq -20\ \text{dB} \\ 0, & \text{if } \frac{(\Gamma_\perp + \Gamma_\parallel)}{2}(\text{dB}) < -20\ \text{dB} \end{cases}$$

Cost 1 is determined by the coating height and Cost 2 is associated with the reflection cost. Both costs are normalized to a value between zero and one. For Cost 2, one denotes an average reflection coefficient of 0 dB while zero denotes an average reflection coefficient that is below -20 dB. The nondominated sorting method [17] is used to combine the two costs for each solution by means of the Pareto ranking. This method assigns rank 1 to the nondominated solutions of the population. The term nondominated solution means that there are no other solutions that are superior to this solution in both objectives. Then the next nondominated solutions among the remaining solutions are assigned rank 2. The process is iterated until all the solutions in the population are ranked. Based on the rank, the same reproduction process described in Section III is performed to refine the population into the next generation. The set of rank 1 solutions is called the Pareto front. In order to avoid the solutions on the Pareto front from converging to a single point in the cost space, we perform a sharing scheme described in [18]. In the sharing process, the rank is modified by penalizing those members on the front that are too close to each other in the cost space. This is accomplished by multiplying a niche count (m_i) to the assigned rank. The niche count is calculated according to

$$m_i = \frac{1}{N_p}\sum_{j=1}^{N_p} Sh(d_{ij}) \tag{4}$$

where the N_p is the number of rank 1 members and the sharing function $Sh(d_{ij})$ is a function of the cost distance between solutions expressed as

$$Sh(d_{ij}) = \begin{cases} 2 - \frac{d_{ij}}{d_{\text{share}}}, & \text{if } d_{ij} < d_{\text{share}} \\ 1, & \text{if } d_{ij} > d_{\text{share}} \end{cases} \tag{5}$$

and

$$d_{ij} = \sqrt{(\text{Cost1}(i) - \text{Cost1}(j))^2 + (\text{Cost2}(i) - \text{Cost2}(j))^2}$$

As we can see, the sharing function increases linearly if the other memberson the front are closer than d_{share} from a chosen member i in the cost space. Consequently, those members that have close-by neighbors in the cost space are assigned lower ranks in the reproduction process.

B. Pareto GA Results

In our Pareto GA, the population size is chosen to be 100. A crossover probability of 0.8%, a mutation probability of 0.1% and a d_{share} distance of 1 is used. Fig. 11(a)–(d) shows the convergence of the solutions for this multiobjective problem (reflection cost versus the height of the profile) as the number of

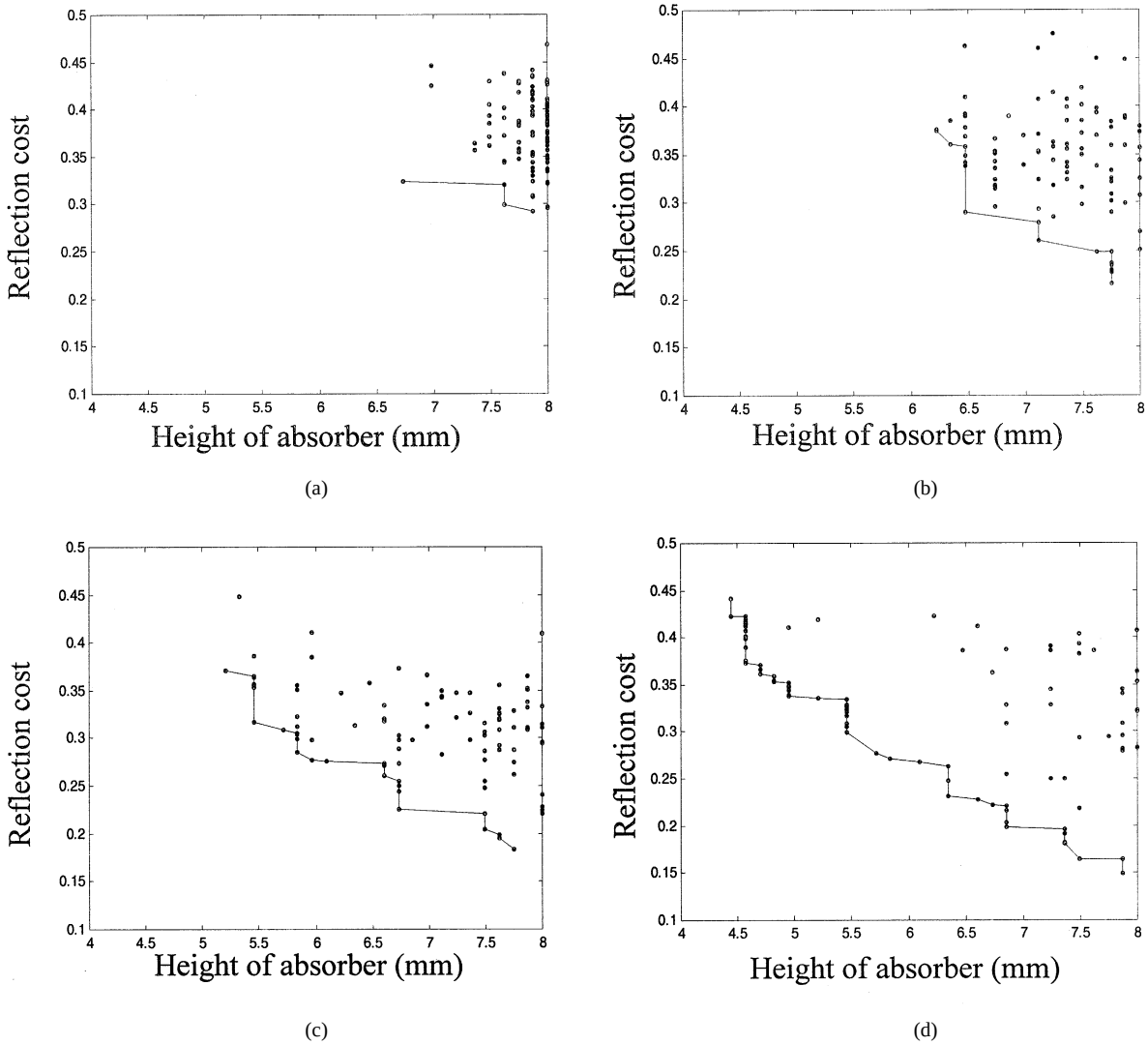

Fig. 11. Convergence of the Pareto front as a function of the number of generations for absorbing performance versus absorber height. (a) Initial population. (b) After five generations. (c) After 20 generations. (d) After 200 generations.

generations is increased. The period of the absorber, the material for the coating, and the angle of incidence are the same as those used in Section III. The height is constrained to be less than 8 mm. Fig. 11(a) is the plot for the initial population. The majority of the solutions is located in the upper right side of the cost domain. Fig. 11(b)–(d) shows plots of the population after 5, 20, and 200 generations, respectively. They show that as the number of generations increases, the Pareto front spreads out and converges toward the lower left region of the cost space. Fig. 12 shows the final converged Pareto front and four optimized coating shapes that are on the front. Inset shape (a) shows the lowest profile of the four samples, but it has the highest reflection among the four designs. Inset shape (d) has the highest profile and the lowest reflection. As expected, the absorbing performance must be traded off against the profile height. If we look in detail at the optimized shapes, we find that as the height of the absorber is decreased, the top of the profile gets more flattened. However, they maintain a rectangular profile that is only slightly modified by the coating height. This is consistent with the physical interpretation of the absorption process for the more dominant horizontal polarization discussed in Section III. Another observation from Fig. 12 is that the Pareto front is not smooth due to the quantization effect of the coating height. If we discretize the height with more binary bits, the shape of the Pareto front becomes smoother.

Next, we try to change the first cost from coating height to coating weight while keeping the reflection cost the same. The cost for the coating weight is normalized to be 1 when all of the design area (period $\times$ maximum coating height) is filled by the coating material while it is zero when no coating material exists. Fig. 13 shows the converged Pareto front for this problem. Also shown in insets (a) to (d) are four optimized shapes with different coating weights. We notice that inset (d) is very similar in shape to inset (d) of Fig. 12. However, instead of trimming the top off in order to reduce the height, the weight consideration results in designs that become progressively skinnier, as shown by insets (c), (b), and (a). Nevertheless, the shapes still preserve the sharp sidewalls as those presented in Fig. 12.

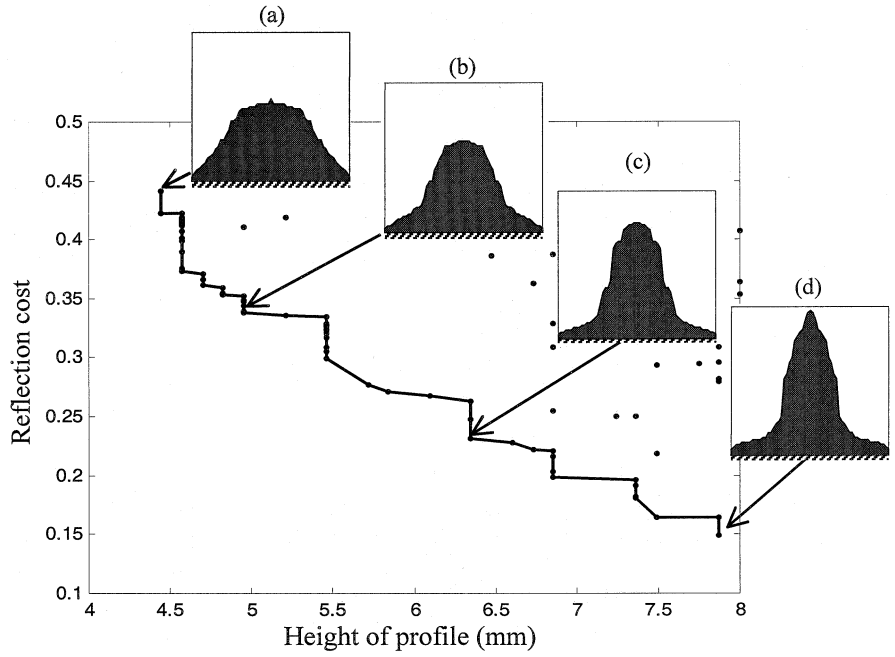

Fig. 12. Final converged Pareto front of absorbing performance versus absorber height. The insets show four sample designs on the Pareto front.

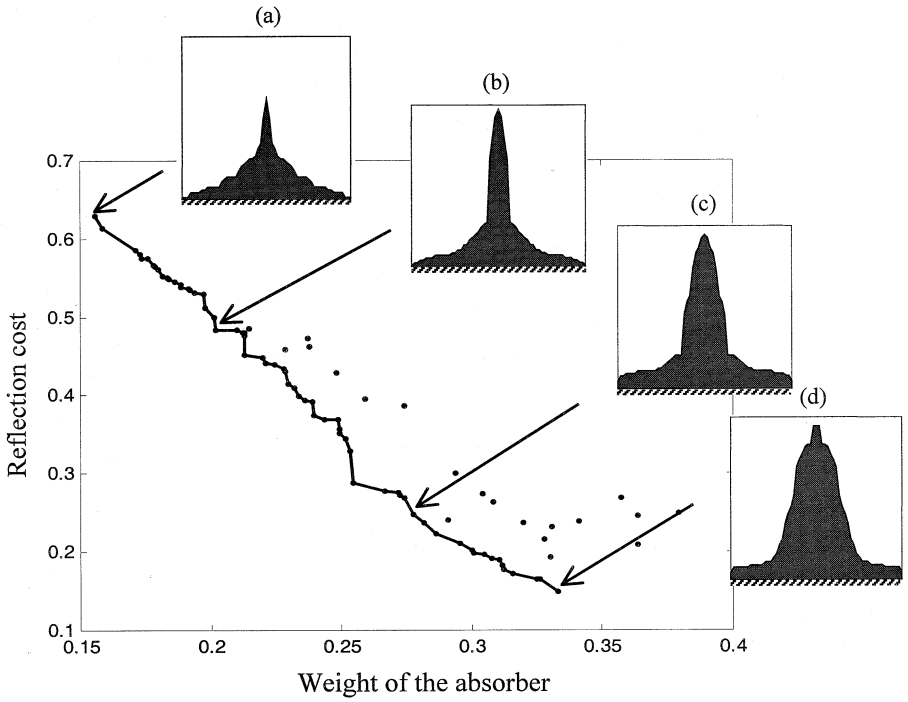

Fig. 13. Final converged Pareto front of absorbing performance versus absorber weight. The insets show four sample designs on the Pareto front.

V. Conclusion

Optimized shapes for a corrugated absorber under near-grazing incidence have been investigated using GA. First, GA was applied to design corrugated coating depending on incident polarizations. The designed absorber shape for the vertical polarization resembled a triangular profile, while that for the horizontal polarization resembled a rectangular profile. The optimized shapes were compared to canonical planar and triangular shaped designs, and were shown to have better absorbing performance. We also tested the sensitivity of the designs to variations in the shape and incident angles, and the result showed reasonable tolerance. A physical interpretation for the optimized shape was presented. It was shown that the

sharp sidewalls of the resulting shape effectively changed the incident polarization from horizontal to the vertical case, thus, facilitating wave absorption.

The Pareto GA has also been applied to efficiently map out absorbing performance versus absorber height. The nondominated sorting method was used to combine the two costs for each solution by means of the Pareto ranking. A sharing scheme was implemented to avoid the solutions on the Pareto front from converging to a single point in the cost space. The converged Pareto front showed that better absorbing performance must be traded off against absorber height. Similar conclusions were also found for the absorbing performance versus absorber weight.

REFERENCES

[1] E. F. Knott, J. F. Shaeffer, and M. T. Tuley, *Radar Cross Section*. Dedham, MA: Artech House, 1985.

[2] J. J. Pesque, D. P. Bouche, and R. Mittra, "Optimization of multilayered antireflection coatings using an optimal control method," *IEEE Trans. Antennas Propagat.*, vol. 40, pp. 1789–1796, Sept. 1992.

[3] E. Michielssen, J. M. Sajer, S. Ranjithan, and R. Mittra, "Design of lightweight, broad-band microwave absorbers using genetic algorithm," *IEEE Trans. Microwave Theory Tech.*, vol. 41, pp. 1024–1031, June–July 1993.

[4] D. Weile, E. Michielssen, and D. E. Goldberg, "Genetic algorithm design of pareto optimal broadband microwave absorbers," *IEEE Trans. Electromagn. Compat.*, vol. 38, pp. 518–525, Aug. 1996.

[5] H. Mosallaei and Y. Rahmat-Samii, "RCS reduction of canonical targets using genetic algorithm synthesized RAM," *IEEE Trans. Antennas Propagat.*, vol. 48, pp. 1594–1606, Oct. 2000.

[6] C. Yang and W. D. Burnside, "A periodic moment method solution for TM scattering from lossy dielectric bodies with application to wedge absorber," *IEEE Trans. Antennas Propagat.*, vol. 40, pp. 652–660, June 1992.

[7] R. Janaswamy, "Oblique scattering from lossy periodic surfaces with application to anechoic chamber absorbers," *IEEE Trans. Antennas Propagat.*, vol. 40, pp. 162–169, Feb. 1992.

[8] C. L. Holloway and E. F. Kuester, "A low-frequency model for wedge or pyramid absorber arrays-II: computed and measured results," *IEEE Trans. Electromagn. Compat.*, vol. 36, pp. 307–313, Nov. 1994.

[9] J. Moore, H. Ling, and C. S. Liang, "The scattering and absorption characteristics of material-coated periodic grating under oblique incidence," *IEEE Trans. Antennas Propagat.*, vol. 41, pp. 1281–1288, Sept. 1993.

[10] J. Moore, H. Ling, C. Liang, and H. Carter, "Oblique scattering from coated periodic surfaces," in *1994 Have Forum Symp. Proc.*, vol. 1, Colorado Springs, CO, Oct. 1994, pp. 283–292.

[11] Dielectric Property of MAGRAM*http://www.arc-tech.com/mag.html* [Online]

[12] H. Choo, H. Ling, and C. S. Liang, "Design of corrugated absorbers for oblique incidence using genetic algorithm," in *IEEE AP-S Symp. Dig.*, Boston, MA, July 2001, pp. 708–711.

[13] D. Goldberg, *Genetic Algorithms in Search, Optimization and Machine Learning*. Reading, MA: Addison Wesley, 1989.

[14] Y. Rahmat-Samii and E. Michielssen, *Electromagnetic Optimization by Genetic Algorithms*. New York: Wiley, 1999.

[15] R. A. Haddad and T. W. Parsons, *Digital Signal Processing*. New York: Computer Science, 1991.

[16] C. L. Holloway and E. F. Kuester, "Power loss associated with conducting and superconducting rough interfaces," *IEEE Trans. Microwave Theory Tech.*, vol. 48, pp. 1601–1610, Oct. 2000.

[17] N. Srinivas and K. Deb, "Multiobjective optimization using nondominated sorting in genetic algorithm," *J. Evol. Comput.*, vol. 2, pp. 221–248, 1995.

[18] J. Horn, N. Nafpliotis, and D. E. Goldberg, "A niched pareto genetic algorithm for multiobjective optimization," in *Proc. 1st IEEE Conf. Evol. Comput.*, vol. 1, 1994, pp. 82–87.

Hosung Choo (S'00) was born in Seoul, Korea, in 1972. He received the B.S. degree in radio science and engineering from Hanyang University in Seoul in 1998, and the M.S. and Ph.D. degrees in electrical and computer engineering from the University of Texas at Austin, in 2000 and 2003, respectively.

From 1999 to 2003, he was a Research Assistant with the Department of Electrical and Computer Engineering, University of Texas at Austin. In September 2003, he joined the School of Electronic and Electrical Engineering, Hongik University, Seoul, Korea, where he is currently a Full-time Instructor. His principal area of research is the use of the genetic algorithm in developing microstrip and wire antennas and microwave absorbers. His studies include broadband and multiband antennas for wireless communications and miniaturized antennas for HF frequency bands.

Hao Ling (S'83–M'86–SM'92–F'99) was born in Taichung, Taiwan, on September 26, 1959. He received the B.S. degrees in electrical engineering and physics from the Massachusetts Institute of Technology, Cambridge, in 1982, and the M.S. and Ph.D. degrees in electrical engineering from the University of Illinois at Urbana-Champaign, in 1983 and 1986, respectively.

He joined the faculty of the University of Texas at Austin in September 1986 and is currently a Professor of Electrical and Computer Engineering and holds the L. B. Meaders Professorship in Engineering. During 1982, he was associated with the IBM Thomas J. Watson Research Center, Yorktown Heights, NY, where he conducted low temperature experiments with the Josephson Department. He participated in the Summer Visiting Faculty Program in 1987 at the Lawrence Livermore National Laboratory. In 1990, he was an Air Force Summer Fellow at Rome Air Development Center, Hanscom Air Force Base. His principal area of research is in computational electromagnetics. During the past decade, he has actively contributed to the development and validation of numerical and asymptotic methods for characterizing the radar cross section from complex targets. His recent research interests also include radar signal processing, automatic target identification, antenna design, and physical layer modeling for wireless communications.

Dr. Ling was a recipient of the National Science Foundation Presidential Young Investigator Award in 1987, the NASA Certificate of Appreciation in 1991, as well as several teaching awards from the University of Texas.

Charles S. Liang (S'64–M'69–SM'93–F'96) received the B.S. degree in electrical engineering from the University of Illinois at Urbana–Champaign, the S.M. degree in applied physics from Harvard University, Cambridge, MA, and the Ph.D. degree from the University of Illinois in 1968.

Since joining the Lockheed Martin Aeronautics Company in 1969, where he is currently a Senior Technical Fellow, he has contributed to the scattering analyses of targets and configuration geometries of practical importance to LO design and to the experimental verification through use of high-resolution radar and coherent imaging system. In addition, he was the principal designer of many rapid-scan antennas used in a series of replica Soviet radars used for aircrew electronic warfare training. In the mid-1970s, he was the resident manager for the successful installation, test, and support of four AN/FPS-110 Aircraft Control & Warning radars in Taiwan, R.O.C. He has been involved in radar systems and signature technology for more than 35 years. In particular, he led the design of the reduced signature F-16 multirole fighter. He was a consultant to both the Tomahawk cruise missile (BGM-109) and the Advanced Cruise Missile (AGM-129) programs. Subsequently, he was responsible for the integration of many low observable (LO) concepts into a unique aircraft configuration that resulted in the A-12 naval medium attack design. Presently, he supports the F-35 Joint Strike Fighter program and other advanced aircraft projects on vehicle signature design and development.

Dr. Liang is a recipient of the 1982 Opal Recognition Award for extraordinary technical performance from General Dynamics and the 1993 Robert E. Gross Award for technical excellence from Lockheed. He was selected to be an Asian American Engineer of the Year 2002 by the Chinese Institute of Engineers/USA. Presently, he is an Associate Fellow of AIAA.